

Electronic Supplementary Information

Fibrilated bacterial cellulose liquid carbene bioadhesives for mimicking and bonding oral cavity surfaces

Juhi Singh^{1,3}, Terry W.J. Steele², Sierin Lim³

¹NTU Institute for Health Technologies, Interdisciplinary Graduate Program, Nanyang Technological University, 61 Nanyang Drive, Singapore 637335

² School of Materials Science and Engineering (MSE), Division of Materials Technology, Nanyang Technological University (NTU), Singapore 639798

³ School of Chemical and Biomedical Engineering, 70 Nanyang Drive, Block N1.3, Nanyang Technological University, Singapore 637457

S1:

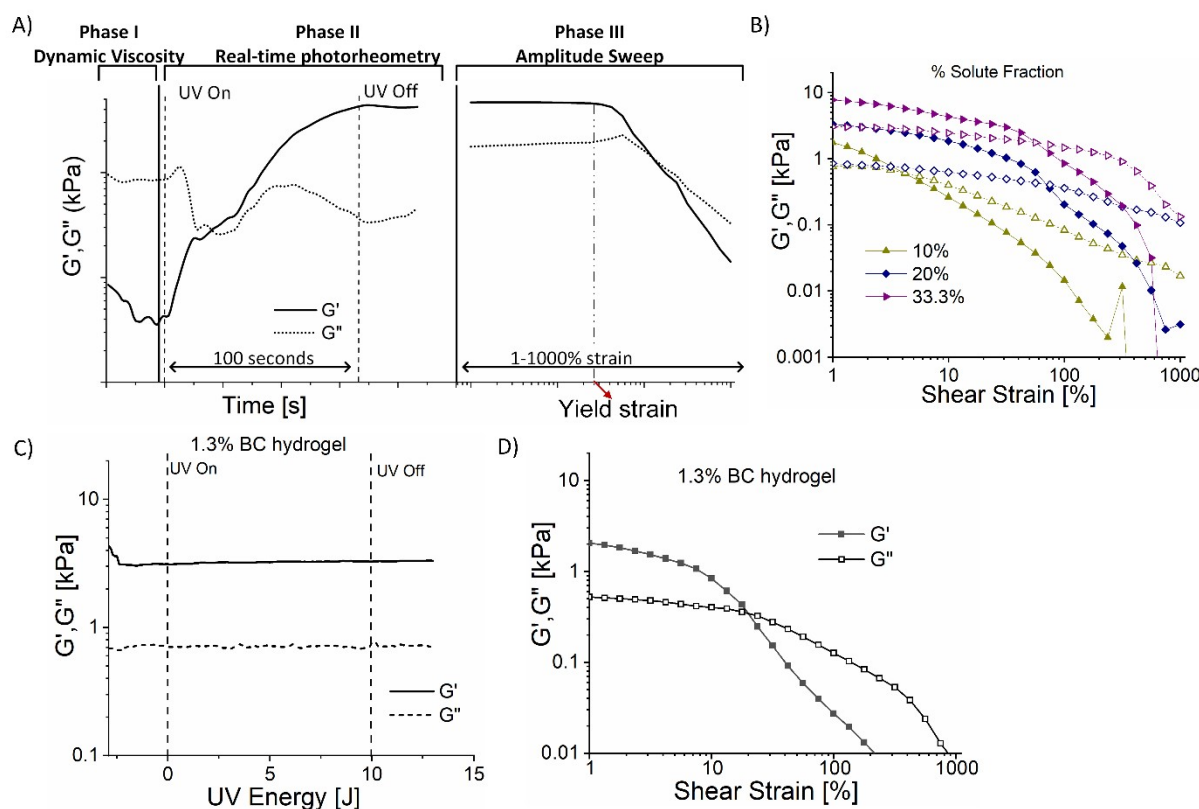


Fig. S1. (A) Photorheological evaluation of composite samples in 3 phases (I) measurement of dynamic viscosity before photocuring (II) measurement of Loss modulus (G'') and Storage modulus (G') as a function of applied UV energy followed by (III) amplitude sweep of cured composites; Rheological properties of BC_PDz(h) composites with varying total solute percentage in the composites (B) Amplitude sweep of photocured BC_PDz(h) composites with increasing total solute percentage in the composites; (C) Photorheogram of 1.3% BC hydrogel depicting changes in Loss modulus (G'') and Storage modulus (G') as a function of applied UV energy up to 10J; (D) Amplitude sweep of 1.3% BC hydrogel.

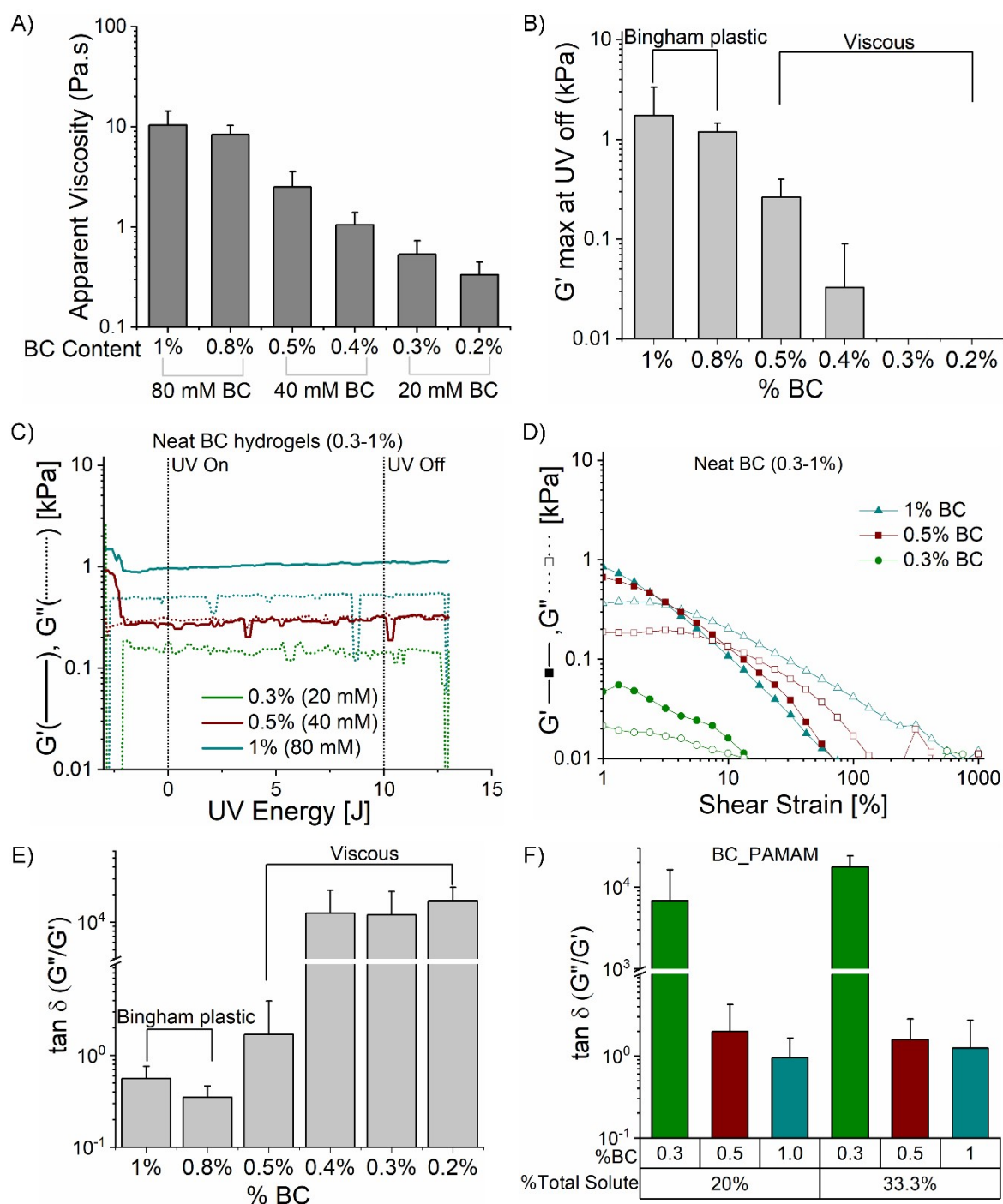


Fig.S2. Rheological properties of neat BC hydrogels with varying %BC (A) apparent viscosity of pre-crosslinked formulations; (B) comparative results of G' maximum measured at UV energy of 10J; (C) representative photorheometry diagrams of dynamic change of G' and G'' during UV exposure in the range of 0–10 J for neat BC hydrogels with 0.3-1%; (D) Amplitude sweep of BC hydrogels after photocuring with neat BC hydrogels with 0.3-1%. (E) comparative results of average $\tan \delta$ measured across 0-10J for neat BC hydrogels (0.2-1%); (F) comparative results of average $\tan \delta$ measured across 0-10J for BC_PAMAM composites with varying %BC for 20 and 33.3% total solute composites. Data presented as mean \pm SD, $n=3$.

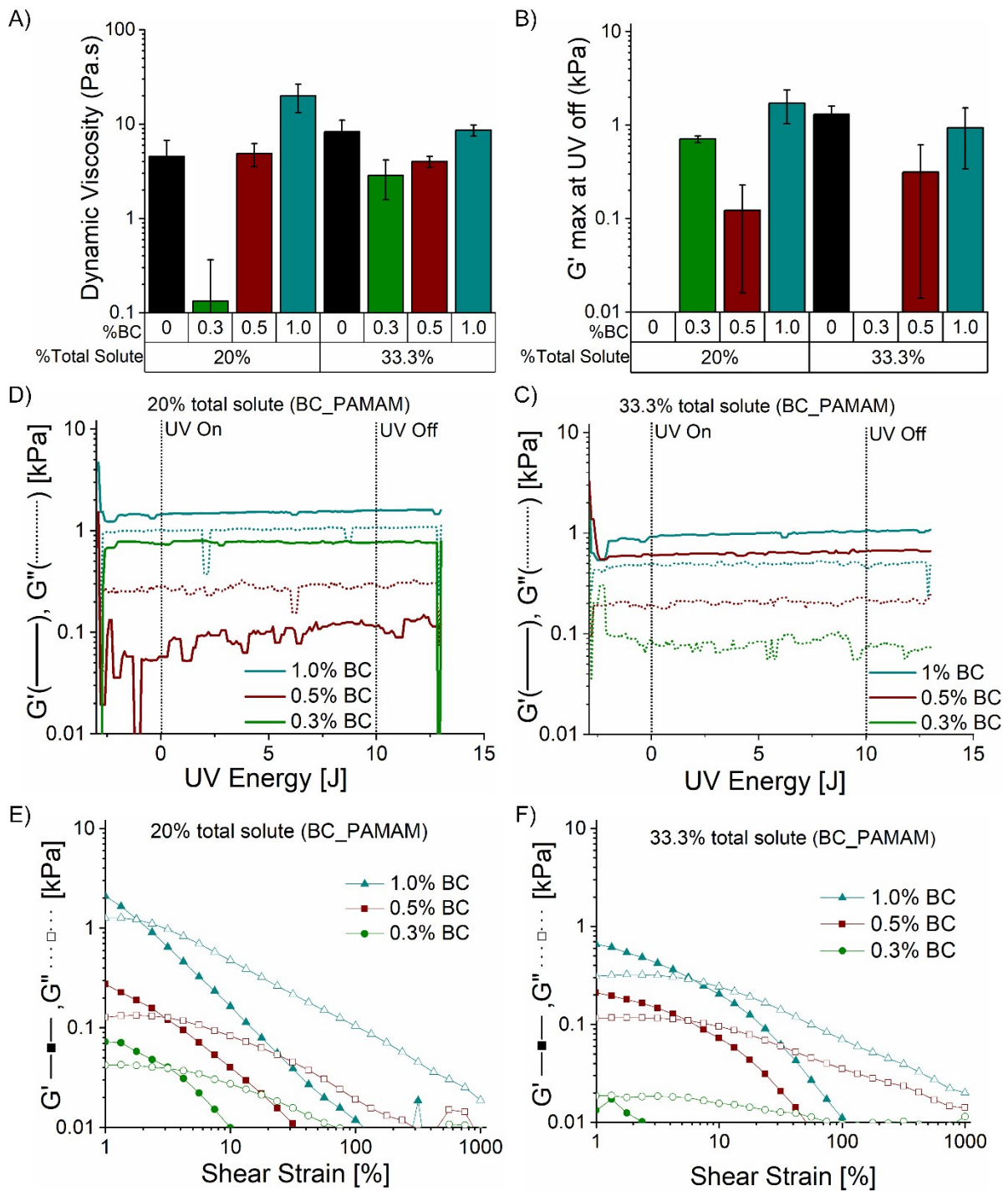


Fig.S3. Rheological properties of BC_PAMAM formulations with varying %BC and total solute percentage (A) Dynamic viscosity of pre-crosslinked formulations; (B) comparative results of G' maximum measured at UV energy of 10J; representative photorheometry diagrams of dynamic change of G' and G'' during UV exposure in the range of 0–10 J (C) 20% total solute;(D) 33.3% total solute; Amplitude sweep of BC hydrogels after photocuring with varying BC % : (E) 20% total solute; (F) 33.3% total solute. Data presented as mean \pm SD, n=3.

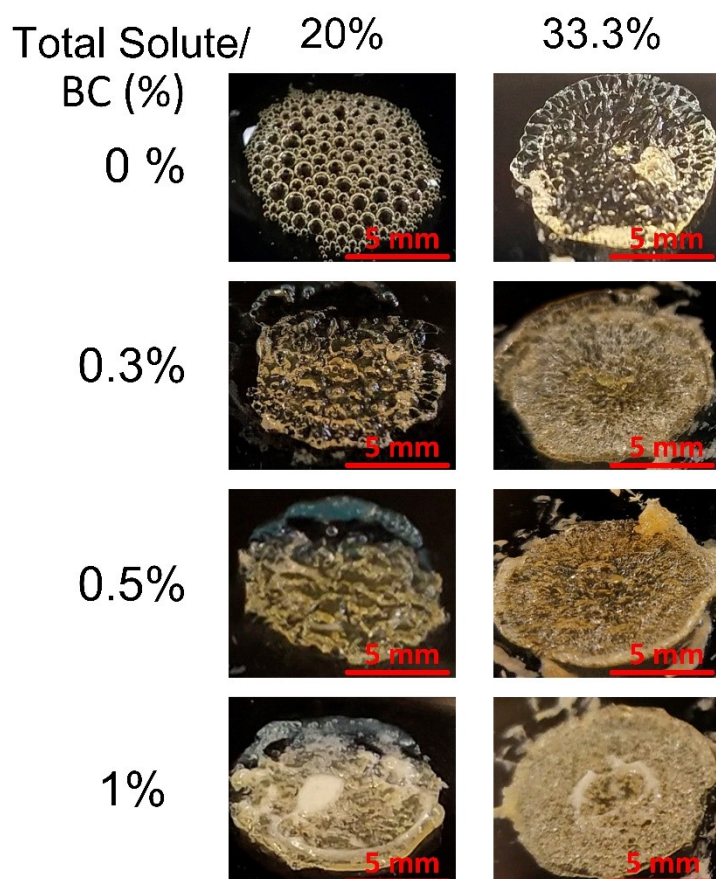


Fig. S4. Images of the photocured BC_PDz(h) composites after completion of III phase of photorheology i.e. amplitude sweep with varying total solute percentage (left to right) and varying %BC (top to bottom).

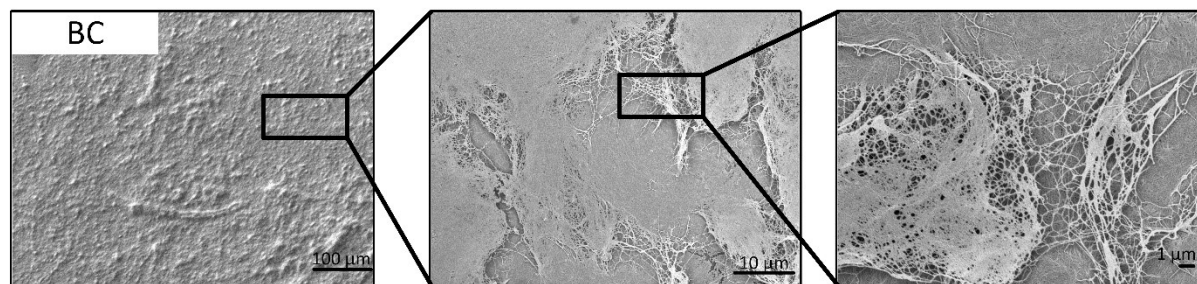


Fig. S5. SEM images of 1.3% hydrogel.

Table S1: Stress at flow point ($G' = G''$) during the amplitude sweep for BC, BC_PAMAM and BC_PDz(h) composites

Total solute % (w/w)	PDz w/w% (mM)	BC w/w% (mM)	[Diazirine]/[OH] mol ratio	Stress at flow point (Pa) (After 10J photocuring)		
				BC	BC_PAMAM	BC_PDz(h)
20	20.0 (6.8)	0.0 (0)	-	-	-	0.3 ± 0.2
20	19.7 (6.8)	0.3 (20)	1.4	1.3 ± 0.7	1.9 ± 0.2	400 ± 100
20	19.5 (6.8)	0.5 (40)	0.7	13.3 ± 5	6.3 ± 1.1	633 ± 153
20	19.0 (6.8)	1.0 (80)	0.35	41.7 ± 26.1	24.0 ± 6.0	443 ± 67
33.3	33.3 (13.6)	0.0 (0)	-	-	-	536 ± 175
33.3	33.0 (13.6)	0.3 (20)	2.8	0.4 ± 0.2	0.4 ± 0.2	966 ± 115
33.3	32.8 (13.6)	0.5 (40)	1.4	4.4 ± 1.7	9.0 ± 0.3	933 ± 152
33.3	32.3 (13.6)	1.0 (80)	0.7	35.2 ± 2.6	25.3 ± 6.3	1233 ± 305

S2: FTIR analysis of cured and uncured BC_PDz(h) composites

FTIR measurements are (PerkinElmer Frontier) performed with Universal ATR fixture of the diamond crystal. Cured and uncured BC_PDz(h) composites are placed directly onto the crystal. Each measurement is an accumulation of 32 scans with a resolution of 4 cm^{-1} and a scan range of 4000 to 600 cm^{-1} .

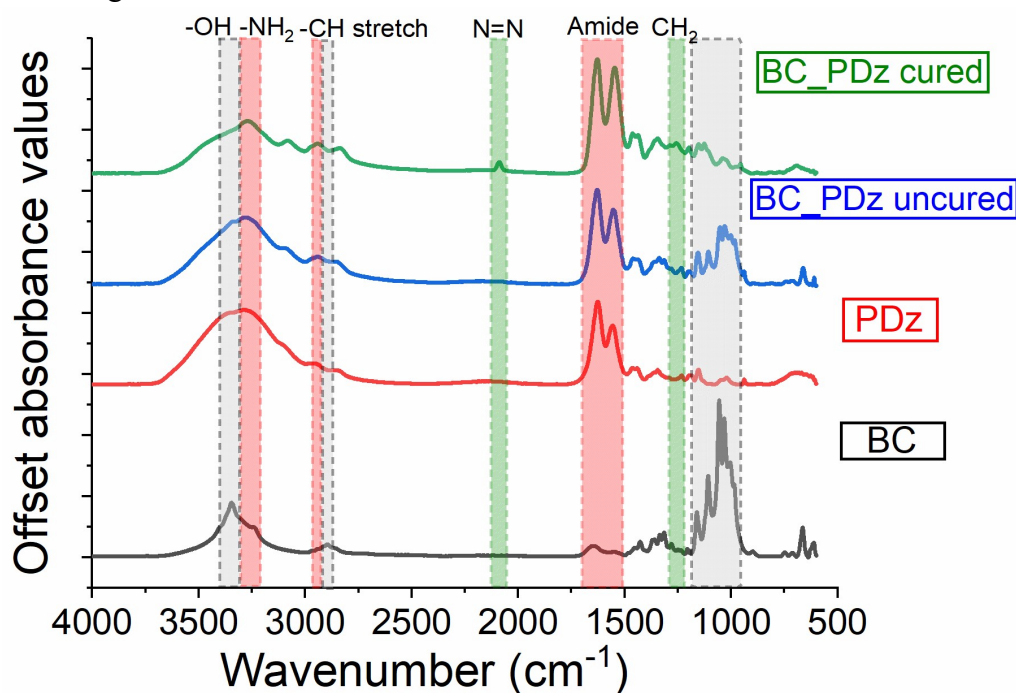


Fig. S6. FTIR spectra of pristine individual components (BC and PDz) and representative BC_PDz(h) before and after UVA based photocuring at 10 J. The peak at 1626 cm^{-1} serves as reference for qualitative peak evaluation.

The primary adhesion mechanism provided by PDz is due to the ability to form carbenes upon UV exposure. In case of BC_PDz(h) composites, it is hypothesized that these carbenes would react majorly with the -OH groups and minorly with -CH- groups present in the bacterial cellulose structure as depicted in **Fig.1**. The FTIR spectra for BC, PDz, uncured BC_PDz(h) composite, and UV cured BC_PDz(h) composites are displayed in **Fig. S6** with associated peak assignments enumerated in **Table S2**. A new peak at 2090 cm^{-1} in the spectra of photocured BC_PDz(h) composite is observed, which corresponds to diazo formation, an intermediate which further lead to formation of carbene radical. Moreover, it is observed that there is a reduction in the absorbance of -CH₂- peak (2938 cm^{-1}), -CH stretch at (2895 cm^{-1}), -OH peak (3345 cm^{-1}), -NH₂ peak (3291 cm^{-1}) and -C-O-H bonds at (1056 cm^{-1}) which supports the carbene insertion mechanism. An increase in the absorbance of ester groups (-C-O-C-) peak (1161 cm^{-1}) and -C-C- bonds peak (1108 cm^{-1}) is observed. An increase in ester group absorbance might be due to the reaction of carbene with -OH groups forming ester and increase in -C-C- bonds due to reaction of carbene with -CH₂ groups as hypothesized in **Fig.1**.

Table S2: FTIR Spectra of 33.3% total solute and 1% BC_PDz(h) before and after photocuring.

FTIR Peak cm^{-1}	Functional Group	Absorbance (Abs)				Normalized Ratio (peak/1626)		
		BC	PDz	BC_PDz (33.3%_1% BC)	BC_PDz cured	BC_PDz (33.3%_1% BC)	BC_PDz cured	%change
3345	-OH stretch	0.18	0.24	0.28	0.17	1.83	0.44	-76
3291	Amine/Hydroxyl	0.12	0.25	0.28	0.20	1.80	0.50	-72
2938	-CH ₂ -	0.03	0.07	0.05	0.11	0.31	0.29	-9
2895	-CH stretch	0.04	0.05	0.04	0.09	0.24	0.23	-5
2090	Diazo	0.01	0.01	0.01	0.05	0.10	0.12	27
1626	Amide I	0.03	0.27	0.15	0.39	1.00	1.00	0
1556	Amide II	0.02	0.19	0.08	0.37	0.50	0.94	88
1280	-CH bending	0.04	0.02	0.01	0.11	0.05	0.28	419
1161	Ester	0.14	0.04	0.03	0.11	0.19	0.29	56
1108	-C-C bonds	0.25	0.00	0.03	0.11	0.21	0.27	26
1056	Bending of -C-O-H bonds	0.50	0.01	0.08	0.08	0.52	0.20	-62
1024	C-O/ C-N	0.32	0.02	0.10	0.07	0.64	0.18	-72

S3:

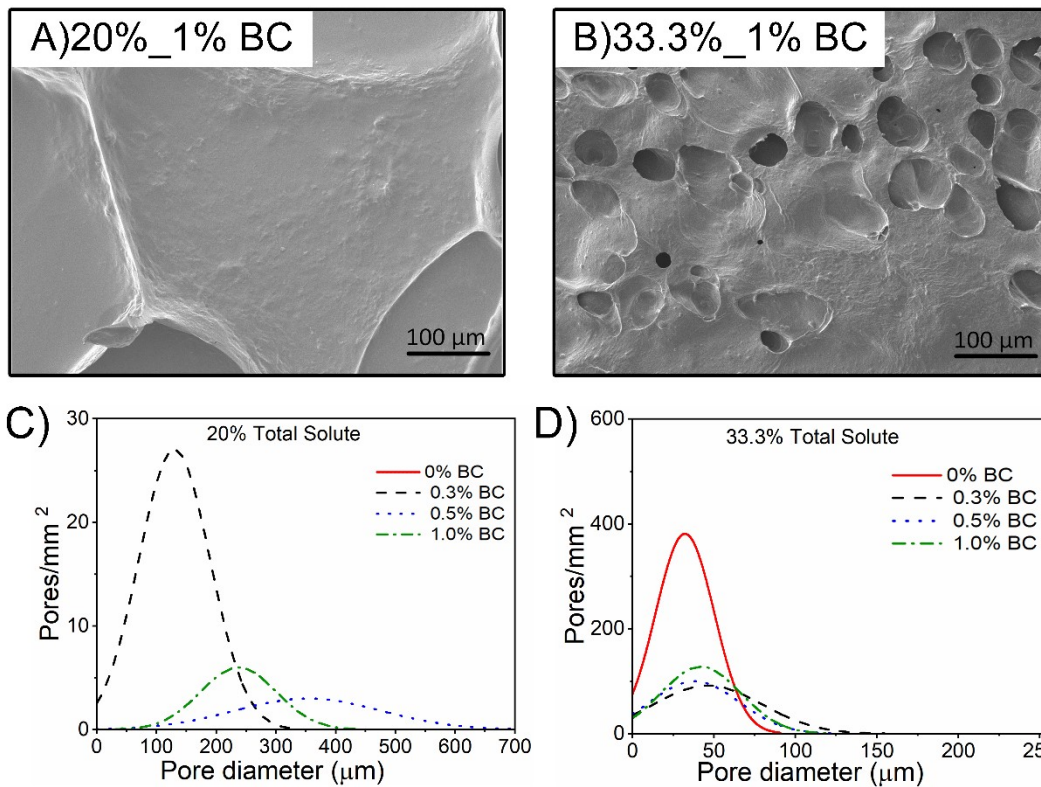


Fig.S7. SEM images of cohesively fractured photocured BC_PDz(h) composite surface (A) 20% total solute, 1% BC; (B) 33.3% total solute, 1% BC; Pore size distribution for cured BC_PDz(h) composites with varying % BC with (C) 20% total solute; (D) 33.3% total solute.

S4:

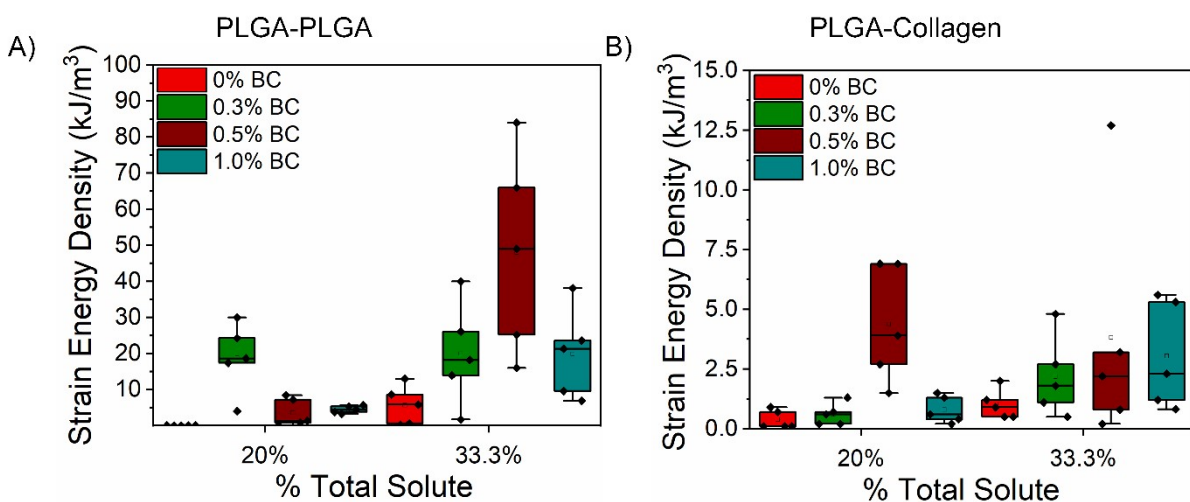


Fig.S8. Strain energy density calculated by integration of stress strain curve (A) 20% total solute (B) 33.3% total solute. Data presented as mean \pm SD, n=5.

S5:

BC_PDz(h) were formulated according to previously used method. The composition in the table 2 with 20 and 33.3% solute percentage and 1% BC was formulated (denoted as native

BC). The hydrogels were freeze-dried to get the dried formulation. The dried formulations were then rehydrated (denoted as Rh BC) with DI water to obtain the formulation with 20 and 33.3% solute. Rheology was performed using the previously used three phase protocol and results were compared to that of original formulations prepared with native BC hydrogel.

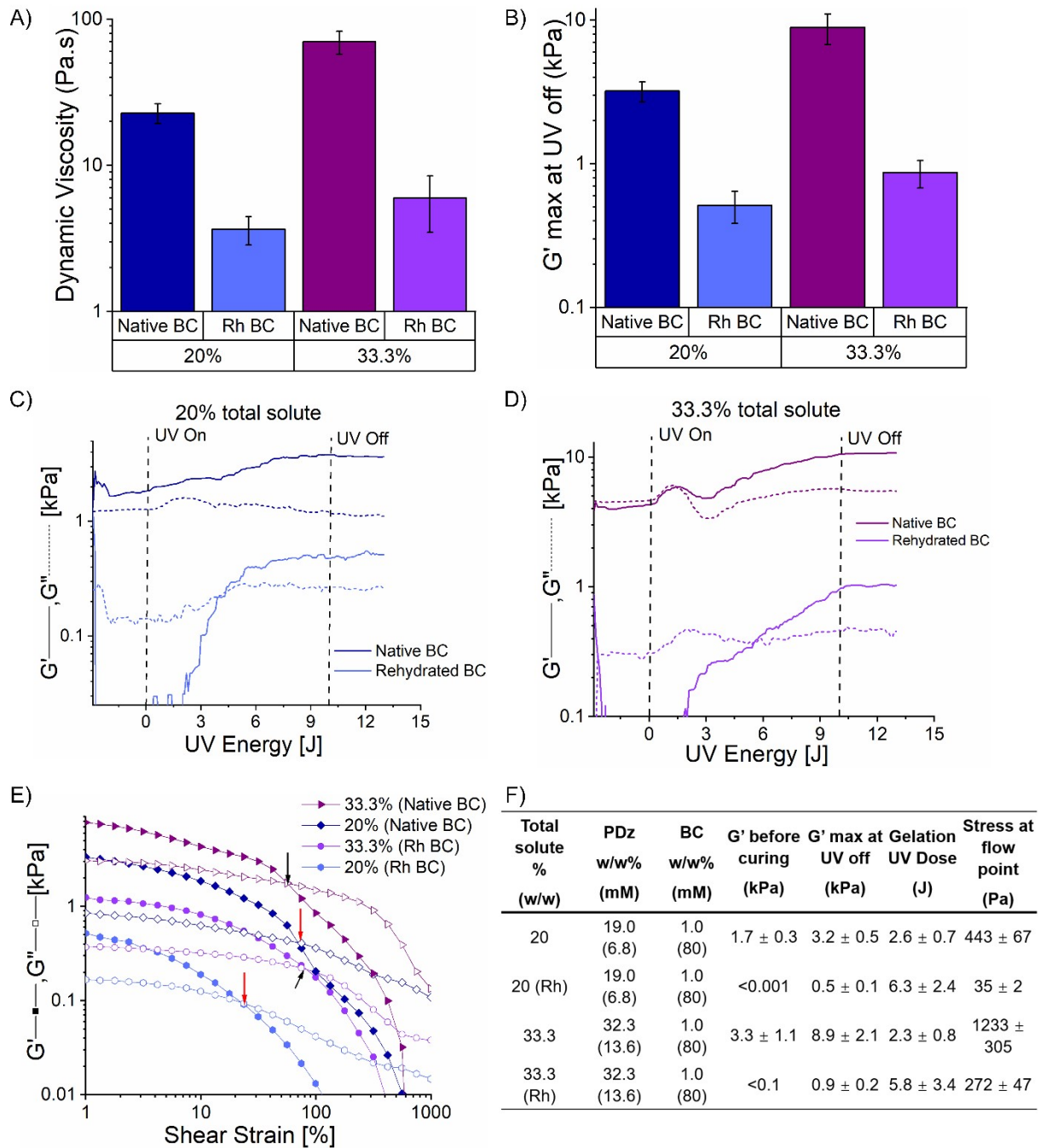


Fig.S9. Rheological properties of BC_PDz(h) composites comprising of native and rehydrated (Rh) BC (A) dynamic viscosity of pre-crosslinked formulations; (B) comparative results of G' maximum measured at UV energy of 10J; representative photorheometry diagrams of dynamic change of G' and G'' during UV exposure in the range of 0–10 J for composites with native and rehydrated BC (C) 20% total solute, 1% BC ; (D) 33.3% total solute, 1% BC; (E) Amplitude sweep of BC_PDz(h) composites after photocuring with native and Rh BC (1%) for 20 and 33.3% total solute. (F) comparative rheological properties BC_PDz(h) composites with native and rehydrated BC. Data presented as mean ± SD, n=3.

S6: Production of PLGA films:

PLGA films are casted using 30% (w/v) PLGA (50:50) solution in DCM (stirred overnight to aid dissolution). The viscous solution is then casted onto flat glass substrate using a knife applicator at 50 mm/sec at room temperature in fume hood. The casted PLGA films are dried at room temperature overnight in the fume hood to prevent foaming. Films are then transferred to vacuum oven and kept for one week for solvent evaporation at 37°C. Thickness of PLGA film was found to be 0.06 ± 0.0039 mm.